J|A|C|S
ARTICLES
Published on Web 06/20/2002

Studying Enzyme Binding Specificity in Acetylcholinesterase Using a Combined Molecular Dynamics and Multiple Docking Approach

Jeremy Kua,* Yingkai Zhang, and J. Andrew McCammon

Contribution from the Howard Hughes Medical Institute, Department of Chemistry and Biochemistry, and Department of Pharmacology, University of California at San Diego, La Jolla, California 92093-0365

Received March 25, 2002. Revised Manuscript Received May 9, 2002

Abstract: A combined molecular dynamics simulation and multiple ligand docking approach is applied to study the binding specificity of acetylcholinesterase (AChE) with its natural substrate acetylcholine (ACh), a family of substrate analogues, and choline. Calculated docking energies are well correlated to experimental k_{cat}/K_M values, as well as to experimental binding affinities of a related series of TMTFA inhibitors. The "esteratic" and "anionic" subsites are found to act together to achieve substrate binding specificity. We find that the presence of ACh in the active site of AChE not only stabilizes the setup of the catalytic triad but also tightens both subsites to achieve better binding. The docking energy gained from this induced fit is 0.7 kcal/mol for ACh. For the binding of the substrate tailgroup to the anionic subsite, both the size and the positive charge of the tailgroup are important. The removal of the positive charge leads to a weaker binding of 1 kcal/mol loss in docking energy. Substituting each tail methyl group with hydrogen results in both an incremental loss in docking energy and also a decrease in the percentage of structures docked in the active site correctly set up for catalysis.

1. Introduction

Substrate binding specificity and catalytic efficiency are intertwined in enzyme catalysis. The enzyme−substrate binding energy lowers the activation energy of k_{cat}/K_M, and there is interconversion of binding and chemical reaction activation energies.[1] Both substrate and protein have to be in the right position to facilitate a low barrier reaction, that is, the orientation of the bound substrate should exert an important effect on enzyme catalysis. Here we demonstrate the applicability of a computational approach, the combination of molecular dynamics simulation and multiple ligand docking, to reveal insight into the structural origins of substrate binding.

Ligand docking is designed to find the best mode of interaction between a small ligand and a large macromolecular receptor. It is one of the most widely used tools in ligand and drug design/screening. In principle, it can provide detailed information not only about how ligands bind to a receptor but also how strongly they bind. In practice, the accuracy of ligand docking depends on the docking score functions and the search algorithm. The recently developed AutoDock 3.0.4 software,[2] used in the present study, has made important advances in both directions. While computational methods for automated docking of ligands to a fixed receptor are both rapid and routine, they do not include the important dynamic behavior of the protein receptor. Methods that do incorporate protein flexibility are gaining importance for their insights into the complex nature of ligand−receptor binding. For recent reviews, see Ma et al.[3] and Carlson and McCammon[4] and references therein.

Molecular dynamics simulation, on the other hand, is a successful and well-established method in the computational study of structure and dynamics of biological macromolecules. Our goal is to show that the proper combination of these two powerful computational tools provides a promising approach to studying enzyme binding specificity, which includes the aspects of binding strength, binding orientation, and ligand−receptor induced fit effects.

The enzyme we have chosen to study is acetylcholinesterase (AChE, EC 3.1.1.7), a serine hydrolase responsible for the termination of impulse signaling at cholinergic synapses. It catalyzes the hydrolysis of the neurotransmitter acetylcholine (ACh) with a remarkably high catalytic efficiency, and is also a promising drug-design target for the treatment of Alzheimer's disease.[5,6] In fact, it is the only target that has provided the few palliative drugs presently marketed for the treatment of Alzheimer's.

The active site of AChE, located at the base of a long and narrow 20 Å gorge,[7] consists of two subsites, an "esteratic" subsite containing the catalytic machinery, and an "anionic"

* To whom correspondence should be addressed. E-mail: jkua@mccammon.ucsd.edu.

(1) Fersht, A. *Enzyme Structure and Mechanism, 2nd ed.*; W. H. Freeman and Company: New York, 1987.
(2) Morris, G. M.; Goodsell, D. S.; Halliday, R. S.; Huey, R.; Hart, W. E.; Belew, R. K.; Olson, A. J. *J. Comput. Chem.* **1998**, *19*, 1639−1662.
(3) Ma, B. Y.; Shatsky, M.; Wolfson, H. J.; Nussinov, R. *Protein Sci.* **2002**, *11*, 184−197.
(4) Carlson, H. A.; McCammon, J. A. *Mol. Pharmacol.* **2000**, *57*, 213-218.
(5) Quinn, D. M. *Chem. Rev.* **1987**, *87*, 955−979.
(6) Giacobini, E. *Cholinesterases and Cholinesterase Inhibitors*; Martin Dunitz Ltd.: London, 2000.
(7) Sussman, J. L.; Harel, M.; Frolow, F.; Oefner, C.; Goldman, A.; L, L. T.; Silman, I. *Science* **1991**, *253*, 872−879.

10.1021/ja020429l CCC: $22.00

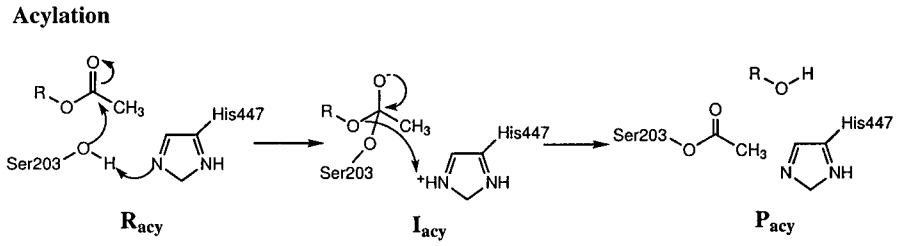

Figure 1. The acylation step in catalysis of ACh.

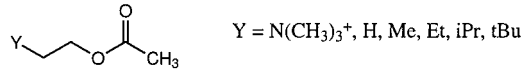

Figure 2. Ligand and ligand analogues of AChE.

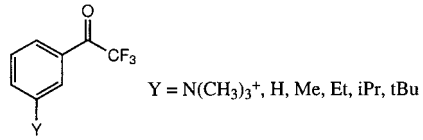

Figure 3. TMTFA inhibitors of AChE.

subsite responsible for binding the quaternary trimethylammonium tailgroup of ACh.[5] The essential catalytic functional unit of AChE is the catalytic triad consisting of Ser203, His447, and Glu334.[5] (*Throughout this article, the sequence numbers follow the amino acid abbreviations of mouse AChE.*) The oxyanion hole, formed by the peptidic NH groups of Gly121, Gly122, and Ala204, is another important functional unit in the esteratic subsite. The X-ray structure of a transition-state analogue complex with *Torpedo californica* AChE[8] revealed that the acetyl headgroup of ACh, directly involved in making and breaking bonds, is held in place by the oxyanion hole. When the acetyl group is held in place, nucleophilic attack from the side chain oxygen of Ser203 to the acetyl carbonyl carbon constitutes the first acylation step (see Figure 1). In the anionic subsite, site-directed mutagenesis indicates that Trp86,[9,10] Glu202,[11] and Phe337[12] play an important role in binding the quaternary trimethylammonium tailgroup. Trp86 and Phe337 are formally thought to bind to the cationic moiety mainly through cation$-\pi$ interactions, while the interaction between Glu202 and the cationic moiety is often attributed to be electrostatic. Recent more detailed mutation studies[10] indicate that the interaction between Trp86 and the quaternary trimethylammonium moiety is approximately evenly split between cation$-\pi$ and dispersion/hydrophobic interactions.

Experimental studies have established that both the esteratic and anionic subsites are responsible for substrate specificity in AChE catalysis. It is found that for a series of substrates, $Y-CH_2CH_2OC(=O)CH_3$, Y=H, Me, Et, *i*Pr, *t*Bu, and N^+Me_3 (as illustrated in Figure 2), the bimolecular rate constant for the reactions catalyzed by AChE, k_{cat}/K_M, follows the trend, H < Me < Et < *i*Pr < *t*Bu < N^+Me_3.[13] Recent experimental binding data of a series of TMTFA transition-state analogue inhibitors, *m*-$YC_6H_4C(=O)CF_3$ (as illustrated in Figure 3, indicate the exact same binding trend of H < Me < Et < *i*Pr < *t*Bu < N^+Me_3.[10]

The present study focuses on investigating the binding specificity of AChE using a combined approach of molecular dynamics simulation and multiple ligand docking. We have performed two 1-ns molecular dynamics simulations, one for apo-AChE, and one for the ACh-AChE substrate−enzyme complex. Multiple docking studies have been carried out by docking ACh, choline, and a family of substrate analogues $Y-CH_2CH_2OC(=O)CH_3$, Y=H, Me, Et, *i*Pr, and *t*Bu to picosecond snapshots of both molecular dynamics trajectories. Our results reveal insight into the structural origins of binding strength, binding orientation, the induced-fit effect, and the possible relationship between binding and catalytic efficiency. Our calculated docking energies are well correlated to experimental k_{cat}/K_M values, as well as to experimental binding affinities of a related series of TMTFA inhibitors.

2. Computational Methods and Procedures

The initial structure was chosen from a snapshot of a 10-ns molecular dynamics simulation of the apo-mAChE with explicit water molecules.[14] The ring of His447 was first rotated into its productive orientation. The apo-enzyme system was then constructed by retaining the whole protein, the sodium cation in the active site, and water molecules within a 24 Å radius of the Ser203 side chain oxygen (Ser203-O). The active site was finally equilibrated by a series of minimizations interspersed with short 20-ps molecular dynamics simulations. This equilibrated structure was the starting structure used for the 1-ns apo-AChE simulation.

The structure of the ACh ligand was constructed in its fully extended conformation according to early experimental and molecular modeling studies.[7,8] The ligand was then optimized using quantum mechanics at the Hartree-Fock level with the 6-31G* basis set.[15] The ligand charges were obtained from electrostatic potential (ESP) fitted charges[16] from the HF/6-31G* quantum mechanics calculation. This procedure was also used in preparing all the ligand analogues and choline for docking.

The ACh-AChE complex was constructed by docking ACh into the equilibrated apo-enzyme simulation using Autodock 3.0.4.[2] The system was further equilibrated with a series of minimizations interspersed by short 20-ps molecular dynamics simulations. This equilibrated structure was the starting structure used for the 1-ns ACh-AChE simulation.

Both 1-ns molecular dynamics simulations were carried out using the TINKER program.[17] Since our focus is on the active site in both

(8) Harel, M.; Quinn, D. M.; Nair, H. K.; Silman, I.; Sussman, J. L. *J. Am. Chem. Soc.* **1996**, *118*, 2340−2346.
(9) Ordentlich, A.; Barak, D.; Kronman, C.; Flashner, Y.; Leitner, M.; Segall, Y.; Ariel, N.; Cohen, S.; Velan, B.; Shafferman, A. *J. Biol. Chem.* **1993**, *268*, 17083−17095.
(10) Quinn, D. M.; Feaster, S. R.; Nair, H. K.; Baker, N. A.; Radic, Z.; Taylor, P. *J. Am. Chem. Soc.* **2000**, *122*, 2975−2980.
(11) Radic, Z.; Gibney, G.; Kawamoto, S.; MacPhee-Quigley, K.; Bongiorno, C.; Taylor, P. *Biochemistry* **1992**, *31*, 9760−9767.
(12) Radic, Z.; Pickering, N. A.; Vellom, D. C.; Camp, S.; Taylor, P. *Biochemistry* **1993**, *32*, 12074−12084.
(13) Hasan, F. B.; Cohen, S. G.; Cohen, J. B. *J. Biol. Chem.* **1980**, *255*, 3898−3904.
(14) Tai, K.; Shen, T. Y.; Borjesson, U.; Philippopoulos, M.; Mccammon, J. A. *Biophys. J.* **2001**, *81*, 715−724.
(15) Hehre, W.; Radom, L.; Schleyer, P.; Pople, J. *Ab Initio Molecular Orbital Theory;* John Wiley & Sons: New York, 1986.
(16) Besler, B. H.; Merz Jr., K. M.; Kollman, P. A. *J. Comput. Chem.* **1990**, *11*, 431−439.
(17) Ponder, J. W. *TINKER, Software Tools for Molecular Design, version 3.6*; the most updated version for the TINKER program can be obtained from J. W. Ponder's World Wide Web site at http://dasher.wustl.edu/tinker.

simulations, only atoms within 20 Å of Ser203-O were allowed to move. A twin-range cutoff method was used to treat the nonbonded interactions,[18] a long-range cutoff of 12 Å and a short-range cutoff of 8 Å. The nonbonded pair list was updated every 20 steps. The time-step used was 2 fs. Bond lengths involving hydrogen atoms were constrained using the SHAKE[19] algorithm. The temperature of the simulations was maintained at 300 K using the weak coupling method with a coupling time of 0.1 ps.[20] The molecular mechanics force field used in the present study was the AMBER95 all-atom force field for the protein[21,22] and the TIP3P model for water.[23]

The ACh ligand, choline, and ligand analogues were docked to 999 snapshots, each 1 ps apart, of both the 1-ns simulations. Water and sodium ions were removed prior to docking. The Autodock 3.0.4[2] program was used for all docking studies. The search method used was the Lamarckian genetic algorithm (LGA) set at level 2 with the top 12 structures reported. The ligands were kept rigid both for computational speed and also because in the 1-ns ACh-AChE simulation ACh remained stable in the extended conformation. For analogues with asymmetrical tailgroups (*i*Pr and Et), all three staggered conformations were docked separately, allowing us to study the different roles of the receptor tail-pocket residues Trp86, Glu202, and Tyr337.

The docking free-energy scoring function used by Autodock is given by:

$$\Delta G = \Delta G_{\mathrm{vdw}} + \Delta G_{\mathrm{hbond}} + \Delta G_{\mathrm{elec}} + \Delta G_{\mathrm{tor}} + \Delta G_{\mathrm{sol}} \qquad (1)$$

Each of the terms is defined as follows:

$$\Delta G_{\mathrm{vdw}} = W_{\mathrm{vdw}} \times \sum_{i,j}\left(\frac{A_{ij}}{r_{ij}^{12}} - \frac{B_{ij}}{r_{ij}^{6}}\right) \qquad (2)$$

$$\Delta G_{\mathrm{hbond}} = W_{\mathrm{hbond}} \times \sum_{i,j} E(t)\left(\frac{C_{ij}}{r_{ij}^{12}} - \frac{D_{ij}}{r_{ij}^{10}} + E_{\mathrm{hbond}}\right)$$

$$\Delta G_{\mathrm{elec}} = W_{\mathrm{elec}} \times \sum_{i,j} \frac{q_i q_j}{\epsilon(r_{ij}) r_{ij}}$$

$$\Delta G_{\mathrm{tor}} = W_{\mathrm{tor}} \times N_{\mathrm{tor}}$$

$$\Delta G_{\mathrm{sol}} = W_{\mathrm{sol}} \sum_{i,j} (S_i V_j + S_j V_i) \exp\left(-r_{ij}^2/2\sigma^2\right)$$

The hydrogen bond term has an angle-dependent directional weight, *E(t)*, based on the angle, *t*, between the probe and the target atom. E_{hbond} is the empirically estimated average energy of the hydrogen bonding of water with a polar atom. The electrostatic term uses a distance-dependent dielectric function to model solvent screening based on the work by Mehler and Solmajer.[24] The torsional term is proportional to N_{tor}, the number of sp^3 bonds in the ligand. In the desolvation term, S_i and V_i are the solvation parameter and the fragmental volume of atom *i*,[25] respectively. All five terms have weighting factors, *W*, obtained by fitting a large set of energetic analyses of ligand−receptor complexes.[2]

(18) van Gunsteren, W.; Berendsen, H.; Colonna, F.; Perahia, D.; Hollenberg, J.; Lellouch, D. *J. Comput. Chem.* **1984**, *5*, 272−279.
(19) Ryckaert, J.-P.; Ciccotti, G.; Berendsen, H. J. C. *J. Comput. Phys.* **1977**, *23*, 327−341.
(20) Berendsen, H. J. C.; Postma, J. P. M.; van Gunsteren, W. F.; DiNola, A.; Haak, J. R. *J. Chem. Phys.* **1984**, *81*, 684−3690.
(21) Cornell, W. D.; Cieplak, P.; Bayly, C. I.; Gould, I. R.; Merz, K. M.; Ferguson, D. M.; Spellmeyer, D. C.; Fox, T.; Caldwell, J. W.; Kollman, P. A. *J. Am. Chem. Soc.* **1995**, *117*, 5179−5197.
(22) Fox, T.; Scanlan, T. S.; Kollman, P. A. *J. Am. Chem. Soc.* **1997**, *119*, 11571−11577.
(23) Jorgensen, W. L.; Chandrasekhar, J.; Madura, J.; Impey, R. W.; Klein, M. L. *J. Chem. Phys.* **1983**, *79*, 926−933.
(24) Mehler, E. L.; Solmajer, T. *Protein Eng.* **1991**, *4*, 903−910.
(25) Stouten, P. F. W.; Frömmel, C.; Nakamura, H.; Sander, C. *Mol. Simul.* **1993**, *10*, 97−120.

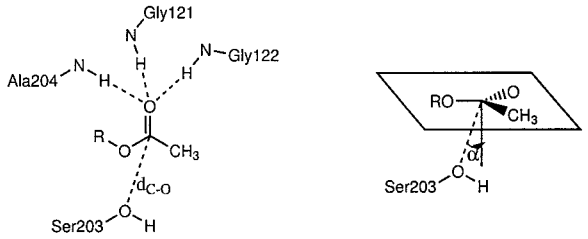

Figure 4. The esteratic binding site for the acetyl headgroup.

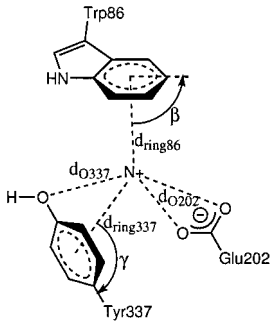

Figure 5. The anionic binding site for the tailgroup.

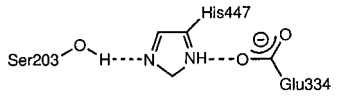

Figure 6. Hydrogen bonds in the setup of the catalytic triad.

In our analysis of the docked structures, we chose only the best docked structure reported by Autodock. A structure is considered to be correctly docked for catalysis if the acetyl headgroup interacts with the oxyanion hole in the esteratic subsite and the tail region is located in the Trp86-Glu202-Tyr337 binding pocket (anionic subsite). The distances and angles used to define the ligand−receptor interactions of docked structures are shown in Figures 4 and 5. We use these same distances and angles in our analysis of the substrate−enzyme interaction in the 1-ns ACh-AChE molecular dynamics simulation.

3. Results and Discussion

3.1. Molecular Dynamics Simulations. Since one of our interests is to examine the interplay between binding and catalysis, we compared the setup of the catalytic triad in both the 1-ns molecular dynamics simulations. The catalytic triad is set up when both Ser203-His447 and His447-Glu334 hydrogen bonds are formed as shown in Figure 6.

For the ACh-AChE complex, both hydrogen bonds are stable throughout the simulation with distances averaging 1.91 (±0.16) and 1.77 (±0.09) Å for the Ser203-His447 and His447-Glu334 hydrogen bonds, respectively. The corresponding N−O distances are 2.83 (±0.12) and 2.75 (±0.08) Å. In the apo-AChE simulation however, only the His447-Glu334 hydrogen bond is stable throughout the simulation. The Ser203-His447 hydrogen bond is only formed part of the time and stable in blocks of 100−200 ps (see Figure 7).

In the catalytic first acylation step, the nucleophilic attack of Ser203-O is accompanied by simultaneous proton transfer from the Ser203-OH group to the ring-N of His447. Since we find that the presence of the ligand serves to stabilize the formation of the Ser203-His447 hydrogen bond, this suggests that ligand binding aids catalysis by the receptor adopting a conformation that favors the proton-transfer reaction.

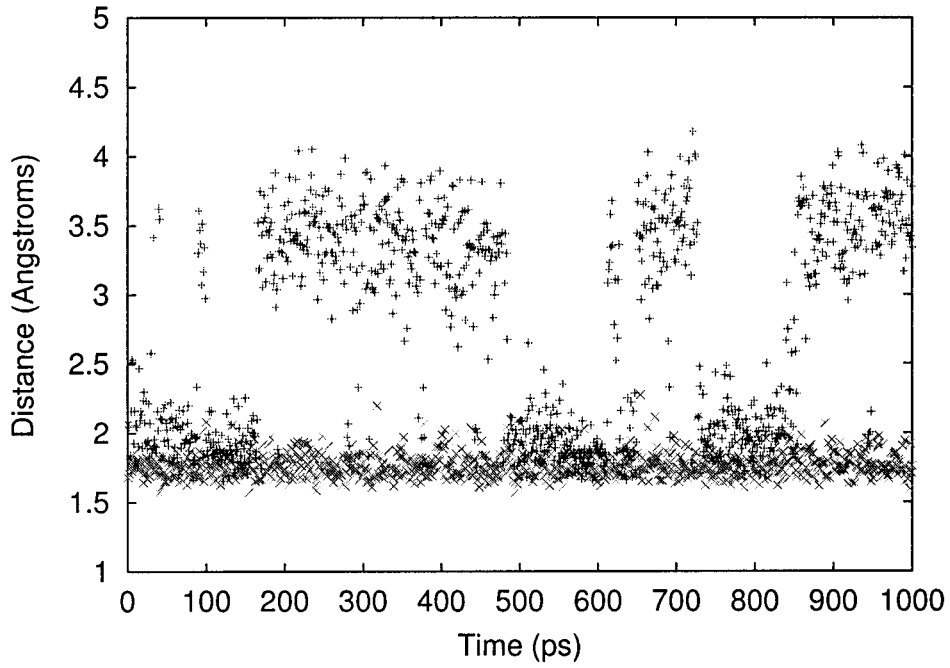

Figure 7. The setup of the catalytic triad along the 1-ns apo-AChE trajectory. The + symbols refer to the Ser203-His447 hydrogen bond, and the X symbols refer to the His447-Glu334 hydrogen bond.

Throughout the entire ACh-AChE simulation, the ACh acetyl headgroup remains close to the oxyanion hole. Two hydrogen bonds are formed between the acetyl carbonyl oxygen and the peptidic NH groups of Gly121 and Gly122 with average N−O distances of 3.01 (±0.18) and 2.92 (±0.13) Å, respectively. Ala204 does not form a hydrogen bond with the average N−O distance being 3.92 (±0.45) Å. The relative position of the acetyl headgroup to these receptor residues is shown in Figure 4. The distance of the carbonyl carbon to Ser203-O, the bond that would be formed in the first acylation step, averages 3.31 (±0.35) Å. The average value of the angle to the normal, α, as shown in Figure 4 is 20 (± 11)°. Best orbital overlap for nucleophilic addition to the sp^2 carbon would be at 0°.

The quaternary trimethylammonium tailgroup remains in the anionic subsite pocket formed by Trp86-Glu202-Tyr337. Distances and angles used to define the position of the tailgroup are shown in Figure 5. The conformation of Trp86 to the quaternary N cation (N^+) suggests a possible cation−π interaction as evidenced by the angle β being close to 90° (calculated average is ∼82°). The average distance of N^+ to the Trp86 six-membered ring is 4.26 (±0.19) Å. Tyr337 prefers the electrostatic interaction between N^+ and the phenol oxygen rather than the cation−π interaction (calculated average of γ is ∼116°). The relative distances of N^+ to the phenol oxygen and to the Tyr337 ring average 4.23 (±0.33) and 4.70 (± 0.28) Å, respectively. The shortest distance comes from one of the carboxyl oxygens of Glu202. The average N^+ distances to the carboxyl oxygens are 4.06 (±0.25) and 5.35 (±0.49) Å, respectively. Plots of the distance and angle changes as a function of time for both head and tailgroups are located in Supporting Information.

We also find that ACh stayed essentially in the extended form throughout the entire ACh−AChE simulation. The four main dihedral angles (as shown in Figure 8) that would contribute to "twisting" of the ligand stayed close to 180°. Figure 9 shows the range of angles sampled by these four dihedrals throughout the course of the simulation. Dihedral 3 has brief twists to ∼90° in the 11−24 and 276−304 ps windows to accommodate a protein conformation that briefly lengthens the distances between Gly121-122 and Ser203-Ala204. This is the distribution line with asterisks in Figure 9. However, these deviations are very short-lived relative to the length of the simulation, and we can conclude that the extended form is both the preferred and stable conformation of the ligand. Subsequently, in our docking studies, we docked ligands rigid in the extended conformation. This has two advantages. First, computational time is greatly reduced, allowing us to sample many protein receptor conformations. Second, the analysis of comparing docking energies of ACh and those of its analogues is now much less complicated, owing to the absence of small conformational twists of the ligand.

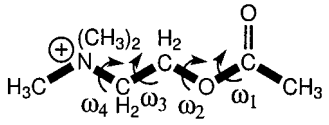

Figure 8. Schematic of dihedral angles along backbone of ACh.

When comparing the relative positions of receptor residues in the binding cavity of the two molecular dynamics trajectories, we find a slight decrease in the active site size during the ACh-AChE simulation which can be attributed to the induced fit effect. More specifically, the oxyanion hole moves closer to Ser203 to form a tighter esteratic subsite, and the Trp86-Glu202-Tyr337 residues close down to form a tighter anionic subsite. The subsites can be illustrated by two triangles as shown in Figure 10. Relevant area sizes and distances are shown in Table 1.

The vertexes of the triangle sweeping out Area1 are at the ring center of Trp86, the phenol oxygen of Tyr337, and the carboxyl oxygen of Glu202 closer to the tail binding site. The vertexes of the triangle sweeping out Area2 are the three backbone nitrogens of the oxyanion hole. *d*1, *d*2, and *d*3, are

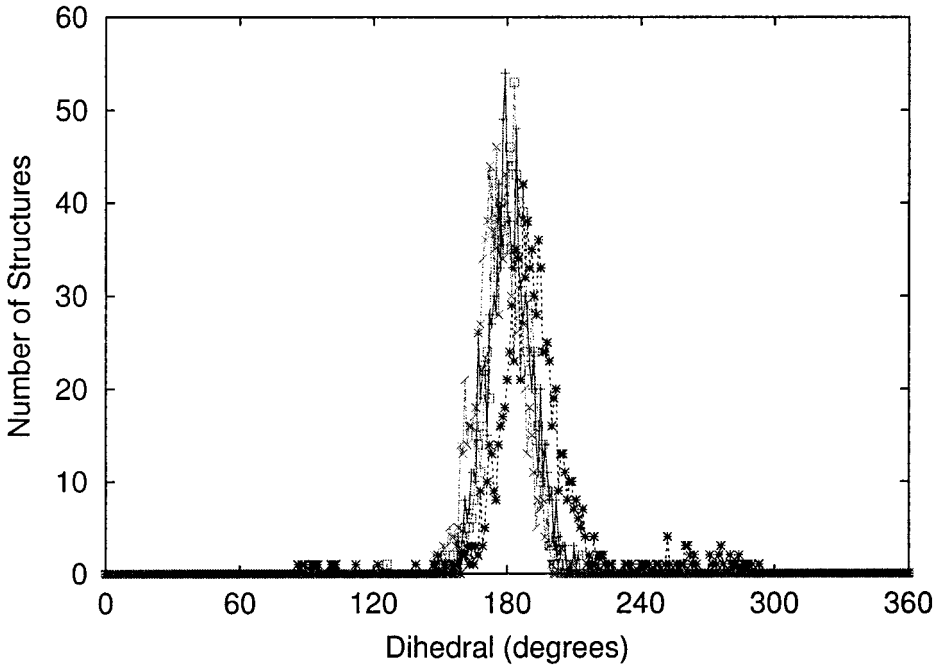

Figure 9. Distribution of backbone dihedral angles in the ACh−AChE trajectory; (+) dihedral ω_1, (×) dihedral ω_2, (*) dihedral ω_3, and (□) dihedral ω_4.

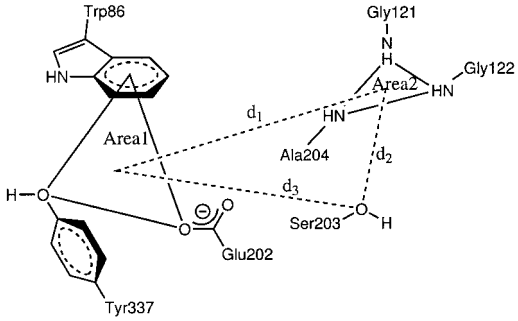

Figure 10. Areas and distances in the binding pocket.

Table 1. Areas and Distances in the Head and Tail Binding Pockets

simulation	Area1 (Å^2)	Area2 (Å^2)	*d*1 (Å)	*d*2 (Å)	*d*3 (Å)
apo-AChE	20.52 (±2.13)	6.72 (±0.27)	6.89 (±0.29)	4.92 (±0.48)	7.92 (±0.51)
ACh−AChE	17.66 (±1.85)	6.59 (±0.29)	6.93 (±0.31)	4.24 (±0.36)	7.44 (±0.37)

Table 2. Number of Structures with Correctly Docked Substrates

	apo-AChE trajectory	ACh–AChE trajectory
N^+Me_3	958	960
*t*Bu	832	990
*i*Pr	763	876
Et	747	834
Me	606	642
H	288	234
choline (tail only)	967	990

Table 3. Average Docking Energies (in kcal/mol) of Correctly Docked Substrates

Y	apo-AChE trajectory	ACh–AChE trajectory
N^+Me_3	−7.10	−7.83
*t*Bu	−6.26	−6.84
*i*Pr	−5.82	−6.17
Et	−5.28	−5.50
Me	−4.79	−4.98
H	−4.35	−4.35
choline	−5.91	−6.03

measured from the center of the two triangles and Ser203-O. From Table 1 we see a decrease in *d*2 of 14% from 4.92 to 4.24 Å when the ligand is present, representing the tighter esteratic subsite. Area1 also decreases by 14% from 20.52 to 17.66 Å^2, representing the closing of the anionic subsite.

Thus, the overall effect of ligand binding is for the protein to tighten both the esteratic and anionic subsites in preparation for catalysis. We shall see in the next section that the docking energy for the binding of ACh to AChE gained from this induced fit is 0.7 kcal/mol.

3.2. Docking Energies and Percentages of Bound Substrates. We find that more than 95% of the best docked ACh structures are correctly docked in the active site to both the apo-AChE and ACh-AChE 1-ns trajectories. In both cases only 36 of the 999 docked structures have neither head nor tail in the correct pockets. For apo-AChE, five structures have the tail correctly bound but not the head; there are three such structures in ACh-AChE. We found no structures that had the head correctly bound but not the tail. The number of correctly docked structures and the average docking energy for each substrate is shown in Tables 2 and 3. The numbers for isopropyl and ethyl are averaged over three conformers. Analysis of the individual conformers is discussed later in this subsection.

The calculated average docking energies for correctly docked structures of ACh to the apo-AChE and ACh-AChE trajectories are −7.10 and −7.83 kcal/mol, respectively. The 0.7 kcal/mol difference represents the gain in ligand−receptor interaction energy due to the induced fit of the receptor in the presence of the ligand.

Comparing the neutral *t*Bu analogue to ACh, we find there is a difference in docking energy of 0.84 kcal/mol between *tert*-butyl and ACh (for apo-AChE, 1.0 kcal/mol for ACh−AChE), reflecting the more favorable intermolecular electrostatic interaction for the charged ligand versus its neutral analogue.

In the family of neutral analogues, reducing the tailgroup size reduces the percentage of correctly docked structures. While *t*Bu has 83% correctly docked in apo-AChE (99% in ACh-AChE), the absence of the tail leads to only ~25% of structures correctly docked. This underscores the importance of having the right-sized tailgroup to bind to the anionic subsite so that the substrate will be in an orientation productive toward catalysis. Except for the analogue with no tailgroup (just hydrogen), the number of docked structures is always higher in ACh-AChE compared to that in apo-AChE.

For the apo-AChE trajectory, the loss in docking energy is in increments of ~0.5 kcal/mol as methyl groups are substituted with hydrogen. The increment is ~0.6 kcal/mol for the ACh-AChE trajectory. Comparing the docking energies of the *t*Bu analogue in both trajectories, the induced fit effect is 0.6 kcal/mol (0.1 kcal/mol less than for ACh). This effect is reduced with decreasing tailgroup size until there is no tail (just hydrogen), where the docking energy for both trajectories is −4.35 kcal/mol. This result is interesting since it indicates that binding just the headgroup alone shows negligible induced fit effect on the docking energy.

We find the same result when the size of the headgroup is reduced. The choline molecule differs from ACh by the replacement of the acetyl headgroup with a hydroxyl group. There was little difference in docking energy of choline to the two trajectories (~0.1 kcal/mol). Binding just the tailgroup alone also shows little effect favoring induced fit. To energetically benefit from induced fit requires the collective effects of binding in both subsites.

Choline, however, has a significantly less negative binding energy than ACh. This is consistent with the effectiveness of AChE as a catalyst in efficiently binding ACh and releasing choline.

Experimental studies indicate that for the series of substrates, the bimolecular rate constant for the reactions catalyzed by AChE, k_{cat}/K_M, follows the trend H < Me < Et < *i*Pr < *t*Bu < N^+Me_3.[13] Recent experimental binding data of a series of TMTFA transition-state analogue inhibitors, *m*-$YC_6H_4C(=O)$-CF_3, indicate the same binding trend.[10] We find that our calculated docking energies also show the exact same trend. Furthermore, as shown in Figures 11 and 12, The calculated docking energies are well-correlated to the experimental k_{cat}/K_M values, as well as to experimental binding affinities of the related series of TMTFA inhibitors.

In ACh and its neutral analogue, the three methyl groups of the tail are each associated with one of the tail binding pocket residues as shown in Figure 13. The number of correctly docked structures of the three ethyl and isopropyl conformers of the neutral analogue and their docking energies are reported in Table 4.

The highest number of successfully docked structures corresponds to maximizing hydrophobic interaction of a methyl group with Trp86 while minimizing with respect to Glu202. Hence ethyl #2 and propyl #1 have the highest percentage of correctly docked structures while ethyl #1 and isopropyl #2 have the lowest. Having a methyl group pointed at Glu202 also prevents the tail from moving closer to Glu202 which indirectly weakens the acetyl head binding in the oxyanion hole, a trend seen in the previous subsection where larger tailgroups also had looser head binding groups. Thus, in terms of docking energies,

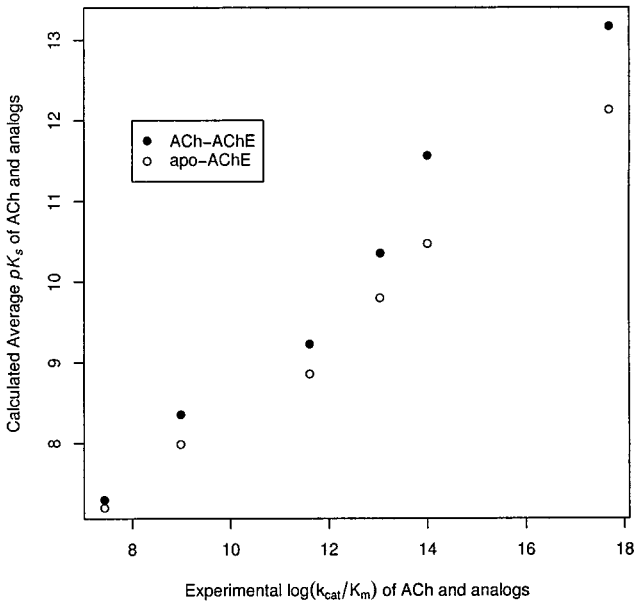

Figure 11. Comparison of calculated ligand pK_s values with experimental $\log(k_{cat}/K_M)$ values, where $pK_s = -(1/RT) \times$ (calculated average docking energy).

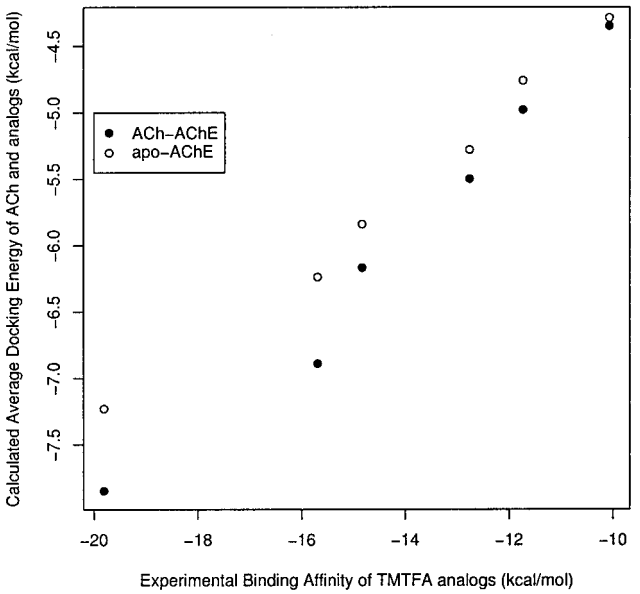

Figure 12. Comparison of ligand analogue docking energies with TMTFA experimental binding energies.

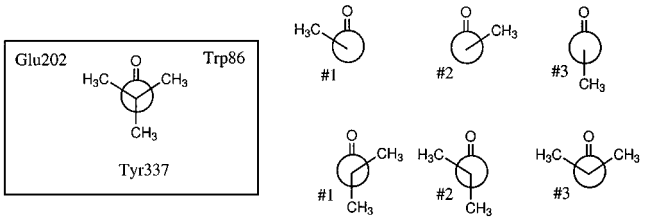

Figure 13. Newman projections of the Et and *i*Pr conformers.

it is not surprising that ethyl #1 binds weakest while isopropyl #1 binds strongest.

3.3. Structural Analysis of Bound Substrates. The important distances and angles for the docked ACh ligand are shown in Tables 5 and 6. In the esteratic subsite, for correctly bound structures, we find two clear hydrogen bond interactions between

Table 4. Docking Energies (in kcal/mol) of Correctly Docked Analogues

	no. of structures	docking energy
apo-AChE trajectory		
ethyl #1	641	−5.19
ethyl #2	859	−5.28
ethyl #3	742	−5.37
isopropyl #1	934	−5.93
isopropyl #2	567	−5.85
isopropyl #3	789	−5.67
ACh−AChE trajectory		
ethyl #1	725	−5.41
ethyl #2	900	−5.45
ethyl #3	876	−5.62
isopropyl #1	997	−6.40
isopropyl #2	707	−6.12
isopropyl #3	923	−5.95

Table 5. Average Distances and Angles of Docked ACh Ligand in the Esteratic Subsite

	no. of struct	acetyl-C Ser203-O (Å)	acetyl-O Gly121-N (Å)	acetyl-O Gly122-N (Å)	acetyl-O Ala204-N (Å)	angle α (deg)
apo-AChE trajectory						
both	958	3.78	2.92	3.00	3.66	18.67
tail	5	7.05	4.24	4.63	6.96	43.36
head	0	–	–	–	–	–
none	36	12.11	8.01	8.89	12.33	95.49
ACh−AChE trajectory						
both	960	2.94	2.85	3.08	3.49	16.30
tail	3	6.98	4.99	5.74	8.09	51.98
head	0	–	–	–	–	–
none	36	10.83	7.94	8.98	12.09	94.37

Table 6. Average Distances and Angles of Docked ACh Ligand in the Anionic Subsite

	no. of struct	d_{ring86} (Å)	d_{O337} (Å)	$d_{O202,1}$ (Å)
apo-AChE trajectory				
both	958	4.50	4.95	3.82
tail	5	3.76	4.58	4.11
head	0	–	–	–
none	36	6.70	5.03	8.33
ACh−AChE trajectory				
both	960	4.52	4.64	3.70
tail	3	4.37	5.13	3.52
head	0	–	–	–
none	36	7.07	5.28	8.00

the acetyl carbonyl oxygen and the peptidic NH groups of Gly121 and Gly122 with N−O distances averaging 2.9−3.1 Å. Recall that this is similar to the results obtained previously in the ACh−AChE simulation where the monitored N−O distances averaged 3.01 and 2.91 Å, respectively. Ala204 does not form a third hydrogen bond. The N−O distance to Ala204 is larger in the apo-AChE simulation, a reflection of the pocket being larger. Similarly, the distance from the acetyl carbonyl carbon to Ser203-O is larger in docked structures to the apo-AChE trajectory. All distances in incorrectly docked ligands are much larger.

In the anionic subsite, the average distances of N^+ to Trp86 and Tyr337 are longer for the docked structures compared to those in the molecular dynamics simulation in the previous subsection. This is balanced by a shorter distance to Glu202.

In the neutral analogue of ACh where *t*Bu replaces the N^+Me_3 tailgroup, the distances in the esteratic subsite are similar

Table 7. Average Distances and Angles of Correctly Docked Analogues in the Esteratic Subsite

	no. of struct	acetyl-C Ser203-O (Å)	acetyl-O Gly121-N (Å)	acetyl-O Gly122-N (Å)	acetyl-O Ala204-N (Å)	angle α (deg)
apo-AChE trajectory						
tert-butyl	832	3.51	3.01	2.84	3.55	32.03
isopropyl	763	3.46	3.04	2.90	3.34	30.83
ethyl	747	3.37	3.03	2.84	3.12	31.08
methyl	606	3.36	3.03	2.82	2.97	32.13
hydrogen	288	3.36	3.00	2.80	2.95	32.43
ACh−AChE trajectory						
tert-butyl	990	2.93	2.80	3.02	3.50	17.46
isopropyl	876	2.92	2.78	3.02	3.45	17.08
ethyl	834	2.91	2.78	3.00	3.37	15.50
methyl	642	2.91	2.76	2.97	3.30	14.66
hydrogen	234	2.88	2.75	2.90	3.13	16.10

Table 8. Average Distances and Angles of Correctly Docked Analogues in the Anionic Subsite

	no. of struct	d_{ring86} (Å)	d_{O337} (Å)	$d_{O202,1}$ (Å)
apo-AChE trajectory				
tert-butyl	832	4.68	4.37	4.20
isopropyl	763	4.67	4.44	4.14
ethyl	747	4.65	4.53	4.02
methyl	606	4.54	4.72	3.92
hydrogen	288	5.11	4.57	3.87
ACh−AChE trajectory				
tert-butyl	990	4.52	4.50	3.83
isopropyl	876	4.54	4.64	3.71
ethyl	834	4.55	5.00	3.43
methyl	642	4.71	5.59	3.16
hydrogen	234	4.79	5.21	3.05

when comparing these two similarly sized substrates. In the anionic subsite the average distances of N^+ to Glu202 and Trp86 are larger for *t*Bu reflecting the decreasing importance of the electrostatic interaction of Glu202 with an uncharged tailgroup. The average N^+ distance to Tyr337 is, however, shorter for *t*Bu. The important distances and angles in the head- and tail binding regions for correctly bound analogues are shown in Tables 7 and 8.

From Table 7, there is increased tightness in the binding of the headgroup reflected by decreases in all four distances as the tailgroup size is reduced. This trend is very clear in the ACh-AChE trajectory but less pronounced in the apo-AChE trajectory. The other important differences between the two trajectories come from the acetyl carbonyl carbon-to-Ser203-O distance and the angle α. Both this distance and angle are considerably larger in the looser pocket of apo-AChE. Note that for correctly docked ACh (discussed in the previous subsection) in the apo-AChE trajectory, this distance is noticeably larger (3.78 Å) but α is only marginally higher (19°).

At the anionic subsite, we see from Table 8 that there is a clear decrease in the shorter d_{O202} distance as the size of the tailgroup is reduced. Both trajectories show this trend. The other two distances (to Trp86 and Tyr337) increase with decreasing tailgroup size in the ACh-AChE trajectory, while the trend is not as clear in the apo-AChE trajectory. Reducing the size of the tailgroup allows more mobility in orienting the substrate in the binding pocket. Rotating the tailgroup toward Glu202 allows a corresponding tighter binding of the acetyl headgroup.

For choline, a correctly docked choline was defined as just having the tailgroup in the anionic subsite. There is no

headgroup to bind to the oxyanion hole. Of the 999 structures, there were 967 and 990 correctly docked choline molecules to the apo-AChE and ACh-AChE trajectories, respectively.

An interesting observation was that the hydroxyl headgroup of the choline was not oriented in the direction preferred by ACh. In fact, more than 75% of the docked structures to apo-AChE had the choline head pointing roughly in the direction of the "back door",[26] close to Tyr449. Since choline is a product of the acylation step in the catalytic reaction, our results suggest the possibility of migration of the choline headgroup toward the back door (while the tail remains in the tail binding pocket) leading to final exit of the molecule via the back door. Migration of the headgroup also opens a pathway for water to hydrolyze Ser203-acetyl, releasing acetic acid (or acetate) in the deacylation step.

4. Conclusions

Multiple docking of ACh and its analogues to apo-AChE and ACh-AChE molecular dynamics trajectories has provided insight into the different factors affecting the binding affinity of ligands in AChE. The calculated docking energies are well-correlated with the experimental k_{cat}/K_M values, as well as with experimental binding affinities of a related series of TMTFA inhibitors. This study demonstrates that the combination of molecular dynamics simulation and multiple ligand docking is a promising computational approach to study enzyme binding specificity.

The comparison between the apo-AChE and ACh-AChE trajectories indicate that the presence of ACh in the active site of AChE not only stabilizes the setup of the catalytic triad but also tightens both esteratic and anionic subsites to achieve better binding. The docking energy gained from this induced fit is 0.7 kcal/mol for ACh. However, either reducing the size of the tailgroup or replacing the acetyl headgroup with hydroxyl (in choline) leads to a negligible induced-fit effect on the docking energy. This is due to the collective effects of both subsites; either on its own has little induced-fit effect on binding.

For the binding of the substrate tailgroup to the anionic subsite, our results confirm that the size and the positive charge of the tailgroup are both important. The removal of the positive charge leads to weaker binding corresponding to a 1 kcal/mol loss in docking energy. Substitution of each tail methyl group with hydrogen results in an incremental loss in docking energy and also decreases the percentage of structures docked in the active site correctly set up for catalysis.

Although the quaternary trimethylammonium tailgroup of choline still binds to the anionic subsite, the hydroxyl headgroup points to the "back door" close to Tyr449. These results are consistent with the experimental fact that AChE can achieve effective catalysis in efficient binding of acetylcholine coupled with efficient release of choline.

Acknowledgment. We are grateful for helpful discussions with Professor Palmer Taylor, Mr. Kaihsu Tai, and Dr. Richard Henchman. This work has been supported in part by grants from the NSF and NIH. Additional support has been provided by NBCR and the W. M. Keck Foundation.

Supporting Information Available: Plots of the distance and angle changes as a function of time for both head and tailgroups (PDF). This material is available free of charge via the Internet at http://pubs.acs.org.

JA020429L

(26) Gilson, M. K.; Straatsma, T. P.; McCammon, J. A.; Ripoll, D. R.; Faerman, C. H.; Axelsen, P. H.; Silman, I.; Sussman, J. L. *Science* **1994**, *263*, 1276−1278.